Hindawi
Journal of Advanced Transportation
Volume 2018, Article ID 3791820, 10 pages
https://doi.org/10.1155/2018/3791820

*Research Article*

# An Improved Single-Lane Cellular Automaton Model considering Driver's Radical Feature

**Xu Qu,[1,2,3] Mofeng Yang ,[3] Fan Yang,[1,2,3] Bin Ran ,[3,4] and Linchao Li[3]**

[1] *Jiangsu Key Laboratory of Urban ITS, Southeast University, No. 2 Sipailou, Nanjing 210096, China*
[2] *Jiangsu Province Collaborative Innovation Center of Modern Urban Traffic Technologies, Southeast University, No. 2 Sipailou, Nanjing 210096, China*
[3] *School of Transportation, Southeast University, No. 2 Sipailou, Nanjing 210096, China*
[4] *Department of Civil and Environmental Engineering, University of Wisconsin-Madison, 1204 Engineering Hall, 1415 Engineering Drive, Madison, WI 53706, USA*

Correspondence should be addressed to Mofeng Yang; yangmofeng@seu.edu.cn

Received 20 November 2017; Revised 28 February 2018; Accepted 14 March 2018; Published 22 April 2018

Academic Editor: Jose E. Naranjo



Traffic flow models are of vital significance to study the traffic system and reproduce typical traffic phenomena. In the process of establishing traffic flow models, human factors need to be considered particularly to enhance the performance of the models. Accordingly, a series of car-following models and cellular automaton models were proposed based on comprehensive consideration of various driving behaviors. Based on the comfortable driving (CD) model, this paper innovatively proposed an improved cellular automaton model incorporating impaired driver's radical feature (RF). The impaired driver's radical feature was added to the model with respect to three aspects, that is, desired speed, car-following behavior, and braking behavior. Empirical data obtained from a highway segment was used to initialize impaired driver's radical feature distribution and calibrate the proposed model. Then, numerical simulations validated that the proposed improved model can well reproduce the traffic phenomena, as shown by the fundamental diagram and space-time diagram. Also, in low-density state, it can be found that the RF model is superior to the CD model in simulating the speed difference characteristics, where the average speed difference of adjacent vehicles for RF model is more consistent with reality. The result also discussed the potential impact of impaired drivers on rear-end collisions. It should be noted that this study is an early stage work to evaluate the existence of impaired driving behavior.

## 1. Introduction

Traffic flow models are fundamental tools to reproduce traffic phenomena and conduct traffic analysis. The microscopic traffic flow models, such as car-following (CF) models and cellular automaton (CA) models, mainly focus on capturing microscopic traffic characteristic. To enhance the performance of the microscopic traffic flow models, numerous factors should be considered. Among these factors, human factors play an important role in recent studies, which can better simulate the effects of driver's driving behavior and individual property, reproducing corresponding traffic phenomena.

Hamdar [1] and Saifuzzaman and Zheng [2] mentioned that human factors should be considered when establishing microscopic traffic flow models, such as reaction time, desired speed, and desired space. At the same time, a series of car-following models and cellular automaton models were established to incorporate these human factors. Wiedemann [3] and Fritzsche [4] both introduced the use of perceptual thresholds into the car-following model (psychophysical model) and a number of researches focused on Wiedemann's model parameter calibration to better describe the driving behavior [5–7]. Fancher and Bareket [8] extended the psychophysical model by introducing a comfort zone. Van Winsum [9] and Wang et al. [10] improved car-following models considering driver's error and distraction. Visual angle and angular speed were taken into account by Anderson and Sauer [11] and Jin et al. [12]. Hamdar et al. [13, 14] modeled driver behavior as a sequential risk-taking task. Besides, the complex driving behavior cellular automaton models were also established based on varieties of driving behaviors. Kerner et al. [15] proposed the KKW model with consideration of speed adjustment behavior in the range of front and rear vehicles. The comfortable driving (CD) model (proposed by Knospe et al. [16]) and its variants cellular automaton models [17–19] all took into consideration the brake light effect, where drivers tended to adopt a more conservative driving behavior when the front vehicle's brake light is on. These models can better capture driver's driving behaviors such as low start and braking behavior and better simulate the traffic flow phenomena.

Among various driving behaviors, drivers' aggressive driving behavior (driver's radical feature) is crucial to the traffic safety studies and greatly affects the stability of traffic flow [20]. In [21], Sharma et al. mentioned that when modeling mixed traffic flow, human factors are always ignored. They categorized aggressiveness or risk-taking propensity as driver's personality traits. Some studies considered driver's radical feature by calibrating the parameters in car-following models and made a simulation using simulation software. Zheng et al. [22] divided drivers into two groups and reproduced driver's radical feature by setting a higher desired speed and changing the driver's lane-changing behavior. Rong et al. [23] and Habtemichael Filmon and de Picado Santos Luis [24] used VISSIM to reproduce the driver's radical feature and made safety implications. Some studies considered driver's radical feature from the model level by modifying traffic flow model: Peng et al. [25] established the timid and aggressive optimal velocity model (TAOVM for short) taking into account both the aggressive and the timid driver's characteristics and tested the linear stability condition. Li et al. [26] discussed the driver's aggressive effects (DAE) by proposing a new lattice model of traffic flow, indicating that DAE can improve the stability of traffic flow in the lattice model. Two two-lane lattice hydrodynamic traffic flow models were proposed by Sharma [27] and Zhang et al. [28] considering the aggressive or timid characteristics of driver's behavior. Zamith et al. [29] introduced a traffic flow cellular automaton model and simulated the difference for daring, standard, and slow drivers as defined. But these studies saw drivers from a group level and evaluated the model by setting the group with a homogeneous radical feature (timid, normal, aggressive, etc.). As mentioned in [21], the differences in the driving behavior under homogeneous conditions, defined as driver heterogeneity, should be incorporated in traffic models to lead to a better understanding of traffic flow phenomena. The individual characteristics of drivers were not presented well. To avoid this problem, Tang et al. [30] improved the full velocity difference model (FVDM) considering driver's behavior by grouping drivers into three categories and discussed driver's individual property; Zhang et al. [31] improved FVDM by considering the acceleration of preceding vehicle and the division of driving types derived from real data. Results showed that the aggressive and regular behavior play a positive role in stabilization of traffic flow while the conservative driver plays a negative role. Cheng et al. [32] proposed an extended continuum model considering aggressive and timid driving behaviors based on FVDM and the result indicated that aggressive behavior can not only suppress congestion but also reduce energy consumption. Kang et al. [33] proposed the Change-CA model that divided drivers to either aggressive or conservative and the property of each driver changes according to initial settings. But the radical degree for individual drivers was not taken into account and thus the driver's individual radical feature cannot be well performed. But except for [31], the parameters of these studies were not calibrated by empirical data.

Based on the CD model and previous studies, this paper innovatively proposed an improved cellular automaton model incorporating driver's individual radical feature (RF model). The radical feature parameter is incorporated in the model from three aspects:

(1) The desired speed of each driver varied considering the driver's individual radical degree calibrated by real world data.

(2) The car-following behavior was changed by modifying the effective distance for drivers with different radical degrees.

(3) The braking behavior of drivers with higher radical degree was less frequent.

Empirical data of a highway segment was used to identify the distribution of driver's individual radical degree and calibrate the parameters of the proposed RF model. Numerical simulation was conducted to validate the superiority of the RF model. Comparison result shows that the RF model is able to reproduce typical traffic phenomena and outperformed the CD model especially in relatively low-density state.

The structure of the paper is organized as follows: Methodology, Results and Discussions, and Conclusions.

## 2. Methodology

*2.1. RF Model Description.* In the actual driving situation, due to gender, age, character, driving skill, and the travel purposes, the desired speed and car-following behavior of individual drivers are diverse. For instance, conservative drivers are prone to adopt a lower driving speed as well as a larger vehicle time headway, while aggressive drivers are the opposite. In traditional cellular automaton models, the desired speed was set to a fixed value for all drivers and the car-following behavior was not able to distinguish the driver's individual property. For this purpose, this research suggests that, in the establishment of a cellular automaton model, the driver's individual radical features cannot be ignored. The proposed cellular automaton model incorporated driver's individual radical feature and was named the RF model.

Driver's radical feature parameter $\alpha_n$ was introduced to measure the radical degree of different drivers. Driver's radical feature was assumed to be subject to the normal distribution in population according to the data acquired from a highway segment. And considering the discretization of the cellular automaton model, the value function of $\alpha_n$ was defined as follows:

$$\alpha_n = \begin{cases} -3 & \text{if } \operatorname{randn}() \le a_1 \\ -2 & \text{if } a_1 < \operatorname{randn}() \le a_2 \\ -1 & \text{if } a_2 < \operatorname{randn}() \le a_3 \\ 0 & \text{if } a_3 < \operatorname{randn}() \le a_4 \\ 1 & \text{if } a_4 < \operatorname{randn}() \le a_5 \\ 2 & \text{if } a_5 < \operatorname{randn}() \le a_6 \\ 3 & \text{if } \operatorname{randn}() > a_6, \end{cases} \quad (1)$$

where randn() is the function that produces a standard normal distribution random number. $a_1$ to $a_6$ are corresponding values when the standard normal function takes a certain cumulative distribution function value. As for driver's radical feature parameter $\alpha_n$, positive values represent the aggressive drivers, negative values represent conservative drivers, and zero value represents drivers who are neither aggressive nor conservative.

Based on the CD model, driver's radical feature parameter $\alpha_n$ was incorporated in the update rules from three aspects.

(1) In order to consider different desired speeds for drivers with different radical degrees, the function of desired speed of the RF model is defined as follows:

$$v_{\max,n} = \overline{v}_{\max+\beta\alpha_n}, \quad (2)$$

where $v_{\max,n}$ is the desired speed of the $n$th vehicle, $\overline{v}_{\max}$ is the average value of all drivers' desired speed, $\alpha_n$ is the driver's radical feature parameter for the driver of the $n$th vehicle, and $\beta$ determines the impact level that $\alpha_n$ has on the desired speed for each driver.

(2) In order to differentiate the car-following behavior of drivers with different radical degrees, the effective distance of the CD model was improved as follows:

$$d_n^{(\text{eff})} = d_n + \max\left(v_{\text{anti}} - \text{gap}_{\text{security}} + \gamma\alpha_n, 0\right), \quad (3)$$

where $d_n^{(\text{eff})}$ denotes the effective gap, $v_{\text{anti}} = \min(d_{n+1}, v_{n+1})$ is the desired speed of the front vehicle, $d_{n+1}$ is the space headway for the $n+1$th vehicle, $\text{gap}_{\text{security}}$ controls the effectiveness of the anticipation, and $\gamma$ is the impact factor that driver's radical feature has on car-following behavior.

(3) The braking behavior of drivers with a higher radical degree is less affected by the brake light of the front vehicle; hence, one more constraint was added to the randomization and braking step of the model:

$$\begin{aligned} &\text{if} && (\operatorname{rand}() < p_{\text{slow}}) \\ &\text{then:} && v_n(t+1) = \max\left(v_n(t+1) - 1, 0\right) \\ &\text{if} && (p = p_b) \\ &\text{then:} && b_n(t+1) = 1 \\ &\text{if} && (\alpha_n > 0) \\ &\text{then:} && b_n(t+1) = 0, \end{aligned} \quad (4)$$

where the braking parameter $p$ is a randomly generated number from 0 to 1. $p_b$ is the probability that will be adopted when the brake light of the vehicle in front is switched on and it is found within the interaction horizon.

The new rule differentiates the driver's braking behavior into two groups. For conservative drivers, they will follow the same rule described in the CD model. For the impaired drivers, their radical feature may lead to their braking behavior being less affected by the front vehicle.

In this way, the desired speed, the driver's car-following behavior, and the braking behavior are associated with the driver's radical feature and presented by the parameter $\alpha_n$. Therefore, the update rules of the proposed model are listed as follows.

*Step 1* (determination of the randomization parameter $p_{\text{slow}}$).

$$p_{\text{slow}} = p\left(v_n(t), b_{n+1}(t), t_h, t_s\right) = \begin{cases} p_b & \text{if } b_{n+1} = 1,\ t_h < t_s \\ p_0 & \text{if } v_n = 0 \\ p_d & \text{in all other cases.} \end{cases} \quad (5)$$

$$b_{n+1}(t) = 0$$

*Step 2* (acceleration).

$$\begin{aligned} &\text{if} && \left(\left(b_{n+1}(t) = 0,\ b_n(t) = 0\right) \text{ or } \left(t_h \ge t_s\right)\right) \\ &\text{then:} && v_n(t+1) = \min\left(v_n(t) + 1, v_{\max,n}\right) \\ &\text{else} && v_n(t+1) = v_n(t). \end{aligned} \quad (6)$$

*Step 3* (braking rule).

$$\begin{aligned} & && v_n(t+1) = \min\left(v_n(t), d_n^{(\text{eff})}\right) \\ &\text{if} && \left(v_n(t+1) = v_n(t)\right) \\ &\text{then:} && b_n(t+1) = 1. \end{aligned} \quad (7)$$

*Step 4* (randomization and braking).

$$\begin{aligned} &\text{if} && (\operatorname{rand}() < p_{\text{slow}}) \\ &\text{then:} && v_n(t+1) = \max\left(v_n(t+1) - 1, 0\right) \\ &\text{if} && (p = p_b) \\ &\text{then:} && b_n(t+1) = 1 \\ &\text{if} && (\alpha_n > 0) \\ &\text{then:} && b_n(t+1) = 0. \end{aligned} \quad (8)$$

*Step 5* (vehicle motion).

$$x_n(t+1) \longrightarrow x_n(t) + v_n(t+1). \quad (9)$$

Here, $b_n$ is the brake light condition of the $n$th vehicle and $b_n = 1$ (0) indicates that the brake light of the $n$th vehicle is on (off). $t_h = d_n / v_{n(t)}$ is the time headway. $t_s = \min(v_{n(t)}, h)$ is the safety time interval, and $h$ is the impact area of the brake light. The deceleration probability follows a rule where $p_b > p_0 > p_d$, which represents the notion that if the front vehicle's brake light is affected, the rear vehicle will decelerate with a larger probability $p = p_b$; when the vehicle's speed is 0, that is, when the vehicle is launching, it will decelerate with an intermediate probability (slow start) $p = p_0$; other cases have a smaller random probability of deceleration $p = p_d$.

It should be noted that the radical feature of each driver is determined by the driver's personal characteristics; that is, the radical degree and the desired speed of each driver are initialized before the simulation and the value of the radical feature parameter will not change as the vehicle location moves after each update.

### *2.2. Model Parameters Calibration*

*2.2.1. Parameter $a_1$–$a_6$ and Parameter $\beta$.* Under a good road condition and when the vehicles' performances are similar, the distribution of the desired speed was thought to be consistent with the distribution of the radical degree in population; hence, the value probability of the driver's radical feature parameter was determined by calibrating the driver's desired speed distribution. Gartner Nathan et al. [34] mentioned that when the space headway is larger than 125 m (approximately equal to 4~6 seconds' time headway with speed 20~30 m/s), vehicles are not in a car-following situation. Therefore, this study posited that, on highway segments with speed limits less than 120 km/h, when time headway is larger than 5 seconds, the driving behavior will not be affected by the front vehicle and the corresponding speed represents the driver's desired speed. To eliminate the possible impact of vehicle performance and roadway condition, this paper collected the traffic flow data from a highway segment under different variable speed limits (VSL), with time headway larger than 5 seconds and the speed interval of 5 km/h.

Tables 1 and 2 show that, under different speed limit conditions, the sum of the percentages of the two speed intervals in the vicinity of the mean desired speed is about 46% to 51% of the total number of vehicles, and the percentage of the next two adjacent speed intervals ranges from 12% to 18% of the total number of vehicles, and the percentage of the next two adjacent speed zones accounts for 5% to 11% of the total number of vehicles, respectively. The percentage of the lowest and highest speed ranges accounts for 2% to 5% of the number of vehicles.

According to the speed distribution discussed above, the probability boundary of radical feature parameter $\alpha_n$ from low to high was set as 3%, 7%, 15%, 50%, 15%, 7%, and 3%, respectively, in this study. And their corresponding values $a_1$ to $a_6$ can be obtained from the normal distribution statistics. Table 3 lists the corresponding values when the standard normal function takes a certain cumulative distribution function value and Figure 1 illustrates the probability density distribution.

Parameter $\beta$ is used to determine the impact intensity that radical feature parameter $\alpha_n$ has on the desired speed. Since the value of radical feature parameter $\alpha_n$ has already been defined, the value of $\beta$ should be able to ensure that the desired speeds for drivers with different radical degrees are consistent with the distribution of real data. According to observations, the speed interval defined by this study is 5 km/h, which is approximately equal to 1 cell; hence, this paper took $\beta = 1$. For example, if $\overline{v}_{\max}$ was set to 23 cells (approximately 124 km/h), the desired speed of the most impaired driver (with $\alpha_n = 3$) will be set as $v_{\max} = 23 + 1 * 3 = 23$ cells (approximately 140 km/h). This distribution is consistent with the observations listed in Table 1.

*2.2.2. Parameter $\gamma$.* Parameter $\gamma$ in the RF model determines the car-following behavior of each driver. The larger the value of $\gamma$, the greater the impact that the radical feature has on the car-following behavior. The difference in car-following behavior will directly influence the traffic volume under medium- and high-density state; that is, it will affect the form pattern of fundamental diagram under medium- and high-density state. Therefore, by simulating the fundamental diagram with different values of parameter $\gamma$ and comparing with the fundamental diagram in the real traffic environment, the appropriate value for parameter $\gamma$ can be calibrated. Due to the lack of suitable real traffic data, this study used numerical simulation to compare the fundamental diagram between the CD model and RF model with different values of parameter $\gamma$. The following process is given as an example to calibrate parameter $\gamma$.

In the simulation, the length of the road was set to 4000 cell units, the time step was set to 1 second, $\overline{v}_{\max}$ was set to 23, and the periodic boundary condition was adopted. The initial location of the vehicle on the road and the initial speed were randomly generated. Parameters $a_1$ to $a_6$ and parameter $\beta$ were set as discussed before. The other parameters are the same as the CD model [16], with a cell length of 1.5 meters, a vehicle length of 5 cells, which is 7.5 meters, $p_b = 0.94$, $p_0 = 0.5$, $p_d = 0.1$, $\text{gap}_{\text{security}} = 7$, and $h = 6$. Other parameters were kept unchanged, and the value of parameter $\gamma$ was gradually changed (this study chose integers from 1 to 5). Each simulation ran 10,600 time steps, of which the first 10,000 time steps did not statistically eliminate the impact of the transient. Each density state was simulated 10 times and the fundamental diagram for CD model and RF model with different values of parameter $\gamma$ could be obtained, as shown in Figure 2.

Figure 2 shows that when the value of parameter $\gamma$ takes 1 or 2, the fundamental diagram in medium- and high-density state is consistent with the CD model. Therefore, parameter $\gamma$ is recommended to take the value of 1 or 2 for this study. This study took $\gamma = 1$. It should be noted that when the RF model is applied to other cases, parameter $\gamma$ should be calibrated by the given real traffic data and the method discussed above should be followed.

## 3. Results and Discussion

In this section, the simulation of fundamental diagram, space-time diagram, and speed differences characteristics was conducted to evaluate the performance of the RF model,

Table 1: The speed distribution of vehicles with time headway larger than 5 seconds on the left lane under different speed limits.

| Speed interval (km/h) | Proportion (%) | | | | |
|---|---|---|---|---|---|
| | 120 km/h (no VSL) | 120 km/h (VSL) | 100 km/h (VSL) | 80 km/h (VSL) | 60 km/h (VSL) |
| <70 | — | — | — | — | 2% |
| 70–75 | — | — | — | — | 7% |
| 75–80 | — | — | — | 4% | 13% |
| 80–85 | — | — | — | 11% | 21% |
| 85–90 | — | — | — | 15% | 25% |
| 90–95 | — | — | 2% | 25% | 17% |
| 95–100 | — | — | 8% | 21% | 10% |
| 100–105 | — | — | 18% | 16% | 5% |
| 105–110 | 4% | 2% | 25% | 6% | — |
| 110–115 | 6% | 5% | 26% | 2% | — |
| 115–120 | 15% | 16% | 12% | — | — |
| 120–125 | 24% | 28% | 7% | — | — |
| 125–130 | 25% | 23% | 2% | — | — |
| 130–135 | 16% | 15% | — | — | — |
| 135–140 | 7% | 8% | — | — | — |
| >140 | 3% | 3% | — | — | — |

Table 2: Mean speed on left lane with time headway larger than 5 seconds under different speed limits.

| Speed limit | 120 km/h (no VSL) | 120 km/h (VSL) | 100 km/h (VSL) | 80 km/h (VSL) | 60 km/h (VSL) |
|---|---|---|---|---|---|
| Mean speed (km/h) | 126.9 | 121.8 | 109.8 | 94.0 | 86.1 |

Table 3: Values for $a_1$ to $a_6$.

| Parameter | $a_1$ | $a_2$ | $a_3$ | $a_4$ | $a_5$ | $a_6$ |
|---|---|---|---|---|---|---|
| Value | −1.88 | −1.28 | −0.68 | 0.68 | −1.28 | 1.88 |

especially compared with the CD model. In the simulation, the length of the road was set to 4000 cell units, and the time step was set to 1 second, and the periodic boundary condition was adopted. The initial location of the vehicle on the road and the initial speed were randomly generated. Each simulation ran 10,600 time steps, of which the first 10,000 time steps did not statistically eliminate the impact of the transient. The value for the new model's parameters is the same as that in the calibration session and the default value for CD model [16].

*3.1. Fundamental Diagram.* This study used 60 seconds as a statistical unit and calculated the average speed of all vehicles for each unit. Each time the simulation can get 10 average speeds under the condition of the chosen density state and the average speed and density can be calculated with the corresponding traffic flow. Each density state was simulated 10 times and the fundamental diagram is shown in Figure 3. Figures 3(a) and 3(b) are scatter fundamental diagrams for the CD model and RF model, respectively; Figure 3(c) is the average flow-density relationship obtained by the ten simulations (each point represents the average value for the ten simulations).

The fundamental diagram of the RF model and the CD model is basically similar in shape like the inversion of the Greek letter $\lambda$ shape. And there is a discontinuity in the intermediate density region; that is, it is possible to simulate the phase change of traffic flow. It can be seen from Figures 3(a) and 3(b) that the main difference between the RF and CD models is the maximum flow (capacity). In the free-flow state, the data points of the CD model are coincident with the same density, while the RF model presents a more dispersed feature in a small range, which is more realistic. It can be seen from Figure 3(c) that the slope of the RF model in the free-flow state is slightly lower than the CD model, indicating that, in the free-flow state, the average speed of RF model is slightly lower than the CD model. Also, the result shows that the maximum flow (capacity) of the RF model is slightly lower than the CD model.

It should be noted that the slight difference of fundamental diagram between the two models is not due to the selected values. The difference in capacity shown in Figure 3(c) is mainly because, in the RF model, drivers with a higher radical degree tend to keep a higher speed and a lower effective distance and follow the front vehicle more closely, which may cause vehicle aggregation phenomenon. Therefore, for the RF model, the braking frequency for the population is larger than CD model, thus causing the decrease of the capacity.

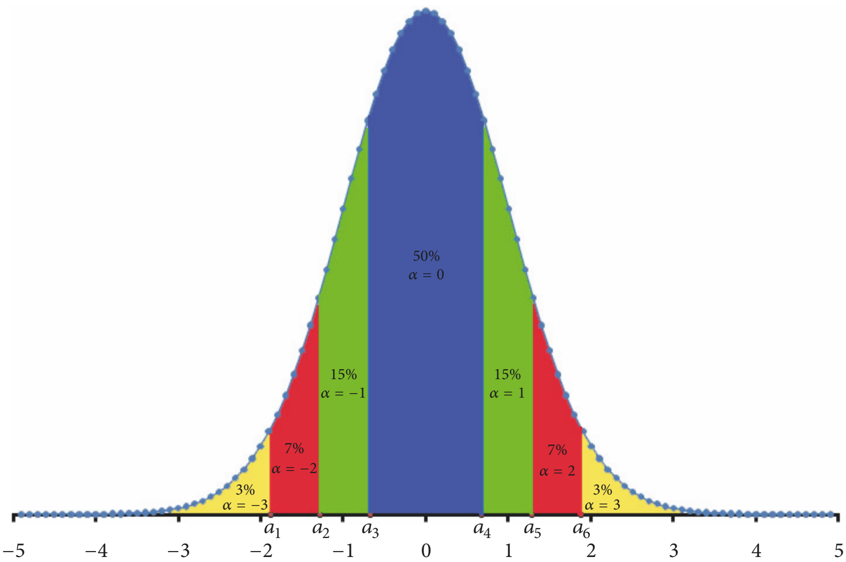


Figure 1: Probability density distribution of a driver with different radical degrees.

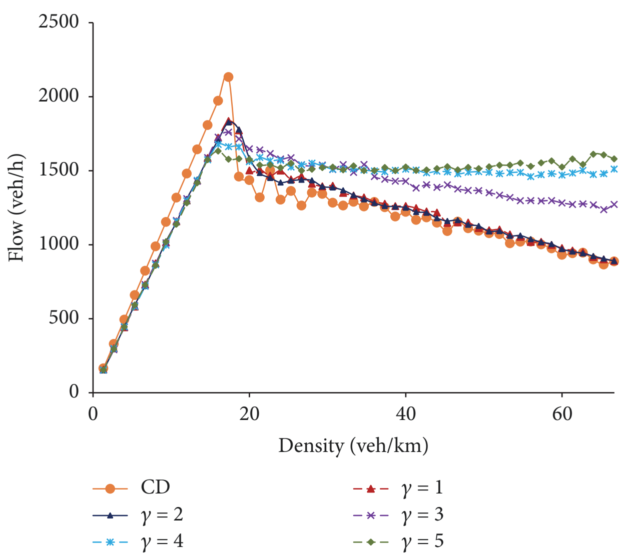


Figure 2: Fundamental diagram generated for parameter $\gamma$ calibration.

*3.2. Space-Time Diagram.* Figure 4 shows the space-time diagram of the RF model and CD model under low (density = 0.1), medium (density = 0.3), and high (density = 0.5) traffic density conditions. The main difference between the two models is, in the low-density state, the space-time diagram of the CD model was an evenly distributed parallel straight line. Figure 4(a) indicates that vehicles are running at a constant speed, and the distance between vehicles is almost constant, with no interference between the vehicles, which is not consistent with the actual situation. Figure 4(b) presents the form of fleet groups, where the vehicle's space-time trajectory is not a strict line and part of the region shows the vehicle aggregation phenomenon, indicating that, in the RF model, the vehicle is not running at constant speed and there exists interference between the vehicles. This is more in line with the real world situation where impaired drivers are willing to follow closely the front vehicle. In medium- and high-density state, the space-time diagrams of the two models have obvious separation of free flow and wide moving jam.

It should be noted that the model proposed in this paper is a single-lane model. On a single-lane road, no matter how radical the driver is, he or she cannot overtake the front vehicle; hence, the phenomenon presented in Figure 4(b) is reasonable under this situation. However, when it comes to two or more lanes, the impaired driver may develop more lane-changing behaviors, especially when he or she catches up with the front vehicle.

*3.3. Speed Difference Characteristics.* The average speed difference (ASD) of two adjacent vehicles was selected to measure the traffic flow speed difference characteristics. It is defined as the mean value of speed difference between the adjacent vehicles passing a given point in a specified time interval [35].

$$\mathrm{ASD} = \overline{\Delta v} = \frac{\sum_{n=1}^{N-1} \left| v_n - v_{n+1} \right|}{n-1}, \tag{10}$$

where $v_n$ represents the speed of the $n$th vehicle passing the fixed point; $N$ represents the number of vehicles passing a given point. In this study, simulations were carried out under different density conditions (10 times for each density) for both RF model and CD model, and the average value of ASD was calculated, as shown in Figure 5.

Figure 5 illustrates that the trend of ASD for the two models is completely different. The ASD of RF model decreases with the increase of density, while the ASD of CD model increases with the increase of density. It can be seen that, in the medium- and high-density state, the difference of ASD for the two models is relatively small. However, in the low-density state, the ASD difference between the two models

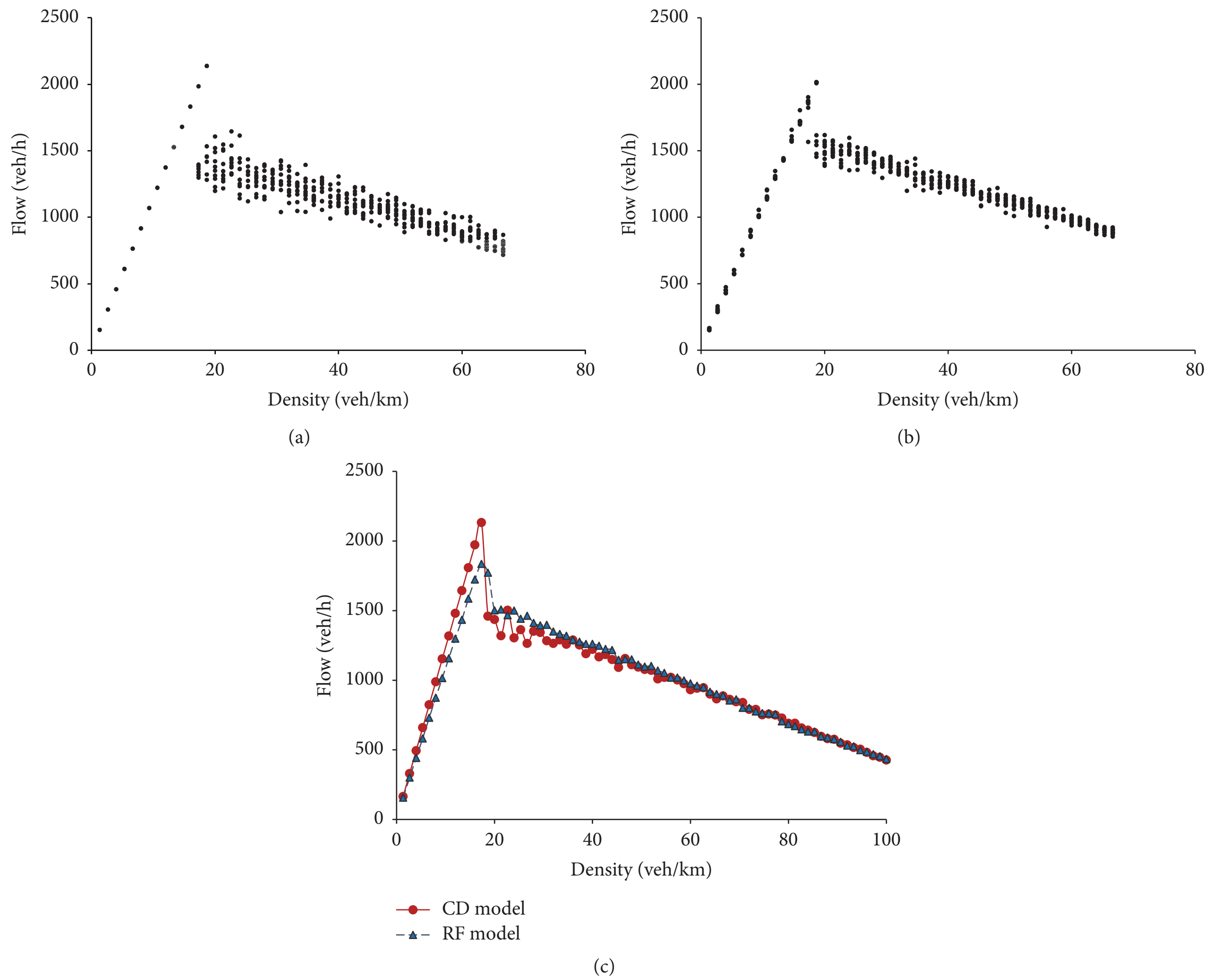


Figure 3: Fundamental diagram of the CD model and RF model. (a) CD model, (b) RF model, (c) and comparison between the CD model and RF model.

is significant. The ASD of CD model was about 1.0 km/h, and the ASD of RF model was about 6.5 km/h. In a previous study for ASD with real traffic data [36], under different speed limits, the ASD has a tendency to decrease with the increase of density and the ASD in low-density state ranges from 6 km/h to 9 km/h. Therefore, the RF model outperformed the CD model in the simulation of speed difference characteristics, which is more in line with the actual situation.

*3.4. Impaired Drivers' Impact on Rear-End Collisions.* The simulation result of speed difference characteristics gives an implication on traffic safety studies. Assuming that there are two vehicles running in the same lane on a motorway, as shown in Figure 6, the leading vehicle is running at the speed of $V_1$, and the following one is running at the speed of $V_2$ with the distance of $d$ from the former. If an emergency happened ahead forcing the leading vehicle driver to brake immediately and adjust its speed to $V_0$ at the deceleration rate of $a$, the following driver also needs to brake to avoid a collision and needs to adjust the speed to at most $V_0$. The following vehicle's deceleration is assumed to be the same as the leading vehicle's, and the drivers' reaction times are ignored.

The distance that the leading vehicle traveled is

$$S_1 = \frac{V_0^2 - V_1^2}{2a}. \tag{11}$$

The distance that the following vehicle traveled is

$$S_2 = \frac{V_0^2 - V_2^2}{2a}. \tag{12}$$

For avoiding a rear-end collision between the consecutive vehicles, the following condition should be met:

$$d > S_2 - S_1 = \frac{V_1^2 - V_2^2}{2a} = \frac{(V_1 - V_2)(V_1 + V_2)}{2a}. \tag{13}$$

Obviously, a rear-end collision would not happen if the speed of the following vehicle ($V_2$) is lower than that of the leading one ($V_1$). However, when the speed relationship is

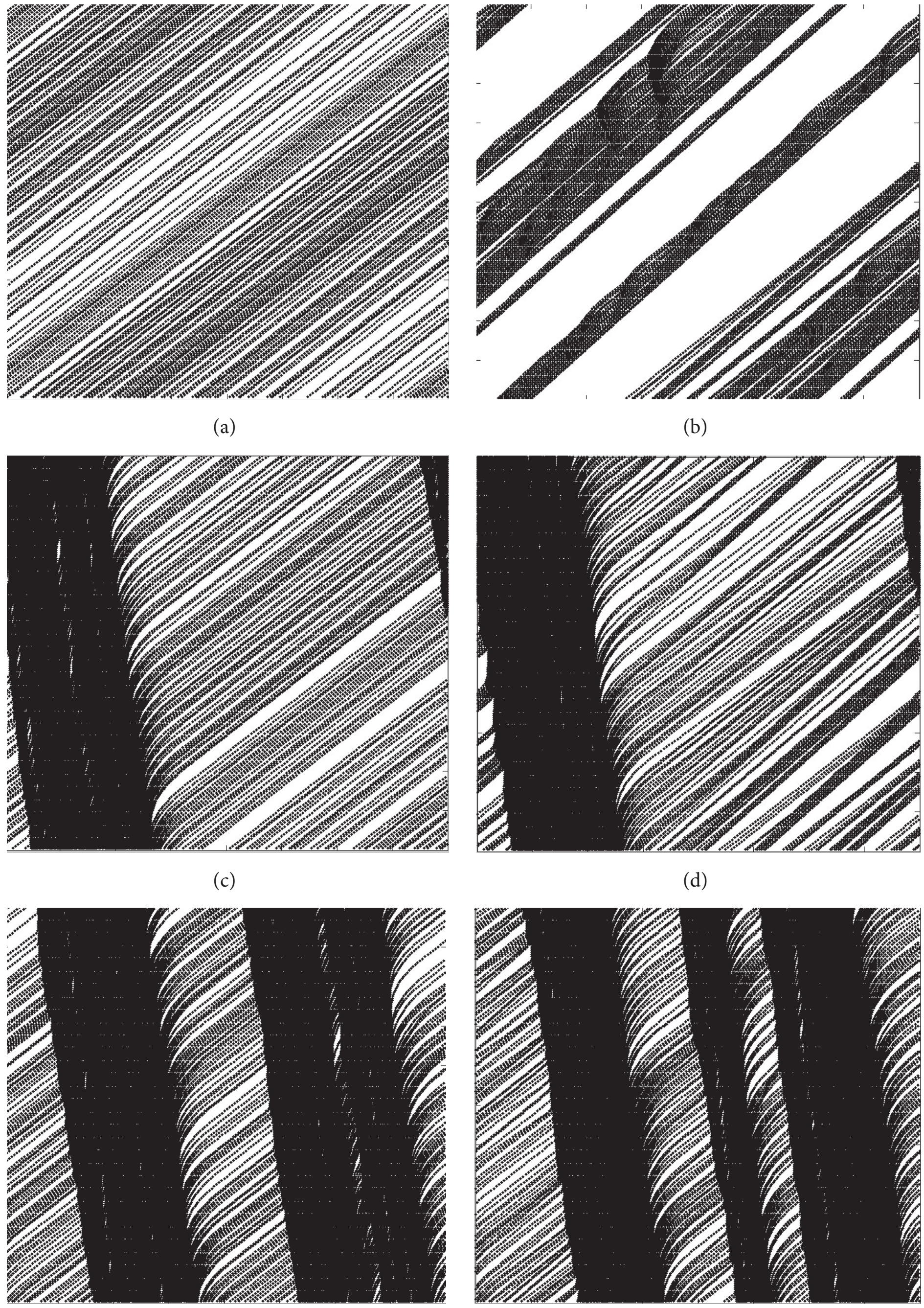

(a) (b) (c) (d) (e) (f)

Figure 4: Space-time diagrams for the CD model and RF model. (a), (c), and (e) are the CD model with density = 0.1, 0.3, and 0.5; (b), (d), and (f) are the RF model with density = 0.1, 0.3, and 0.5.

reversed, whether the collision would occur will depend on the distance ($d$), the speed difference between the adjacent vehicles ($V_2 - V_1$), the sum of the speeds of the two vehicles ($V_2 + V_1$), and the deceleration rate ($a$). It is hypothesized that the deceleration rate of all drivers is of the same value. When a moderate driver is followed by an impaired driver, there will be an increase in both ($V_2 - V_1$) and ($V_2 + V_1$), resulting in a higher risk of rear-end collisions. According to Figure 5, it can be inferred that the existence of both impaired drivers and conservative drivers may deteriorate the traffic safety status. Appropriate VSL controls at places where the drivers show a higher radical degree can decrease the risk of rear-end collisions.

## 4. Conclusions

In summary, on the basis of the CD model, an improved cellular automaton model (RF model) was proposed to

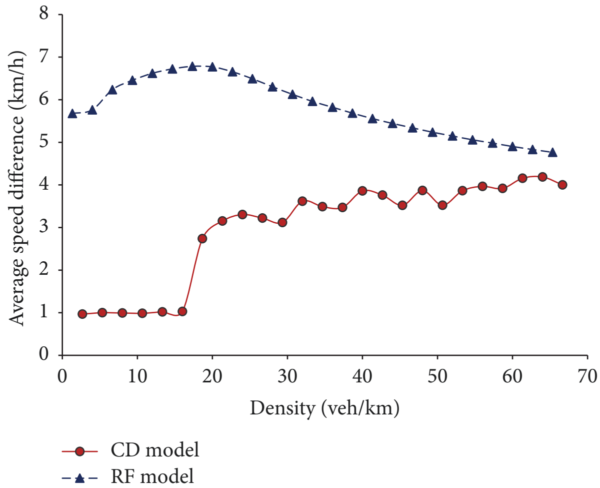


FIGURE 5: Average speed difference of adjacent vehicles simulated by two models.

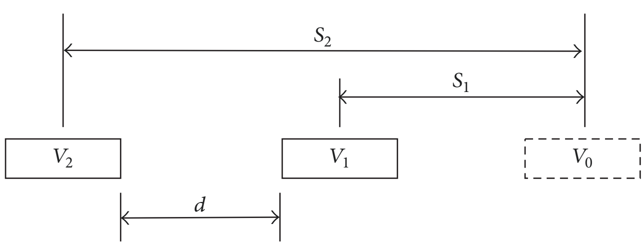


FIGURE 6: Schematic diagram of rear-end collisions.

investigate the effects of driver's individual radical feature on traffic flow characteristic. In the new model, parameter $\alpha_n$ was used to represent driver's individual radical feature and was added to the update rules of the model from three aspects:

(1) Different desired speeds for drivers with different radical degrees.

(2) Different car-following behaviors for drivers with different radical degrees.

(3) Different braking behaviors for drivers with different radical degrees.

Empirical data on a highway segment was used to identify the distribution of driver's individual radical degree and calibrate the parameters of the RF model. The calibration method and the recommended value of the model parameters were also given. Finally, the performance of the new model was evaluated by numerical simulation of the traffic characteristics presented by fundamental diagram, space-time diagram, and speed difference characteristics. The result shows that, in high-density state, the simulation capability of the new model is similar to that of the CD model, while in low-density state, especially for speed difference characteristics simulation, RF model is more realistic than CD model, which shows greater speed difference between vehicles and higher risk of rear-end collisions. This suggests that the new model is more suitable for traffic safety-related studies considering relevant characteristics.

It should be noted that this study assumed that driver's radical feature is subject to normal distribution when defining the function of radical feature parameter. Whether this assumption is reasonable or not needs to be discussed further in future research. Also, this study is just an early stage work to incorporate impaired driving behavior. More works should be done to develop a more accurate calibration process as well as multiple lanes models. In our future research, we will focus on collecting real data to help discuss driver's radical distribution under car-following state.

## Conflicts of Interest

The authors declare that there are no conflicts of interest regarding the publication of this article.

## Acknowledgments

The authors would like to acknowledge the support of the National Science Foundation of Jiangsu Province (Grant no. BK20160685) and the National Natural Science Foundation of China (Grant no. 61620106002).

## References

[1] S. Hamdar, "Driver Behavior Modeling," in *Handbook of Intelligent Vehicles*, A. Eskandarian, Ed., pp. 537–558, Springer, London, 2012.

[2] M. Saifuzzaman and Z. Zheng, "Incorporating human-factors in car-following models: a review of recent developments and research needs," *Transportation Research Part C: Emerging Technologies*, vol. 48, pp. 379–403, 2014.

[3] R. Wiedemann, "Simulation Des Strassenverkehrsflusses," *Institut Fur Verkehrswesen Der Universitat Karlsruhe*, 1974.

[4] H.-T. Fritzsche, "A Model for Traffic Simulation," *Traffic Engineering + Control*, vol. 35, no. 5, pp. 317–321, 1994.

[5] B. Park and H. Qi, "Microscopic simulation model calibration and validation for freeway work zone network - A case study of VISSIM," in *Proceedings of the IEEE Intelligent Transportation Systems Conference*, pp. 1471–1476, 2006.

[6] I. Ištoka Otković, T. Tollazzi, and M. Šraml, "Calibration of microsimulation traffic model using neural network approach," *Expert Systems with Applications*, vol. 40, no. 15, pp. 5965–5974, 2013.

[7] N. E. Lownes and R. B. Machemehl, "Sensitivity of simulated capacity to modification of VISSIM driver behavior parameters," *Transportation Research Record: Journal of the Transportation Research Board*, vol. 1988, pp. 102–110, 2006.

[8] P. S. Fancher and Z. Bareket, "Evolving model for studying driver-vehicle system performance in longitudinal control of headway," *Transportation Research Record*, no. 1631, pp. 13–19, 1998.

[9] W. Van Winsum, "The human element in car following models," *Transportation Research Part F: Traffic Psychology and Behaviour*, vol. 2, no. 4, pp. 207–211, 1999.

[10] W. Wang, W. Zhang, H. Guo, H. Bubb, and K. Ikeuchi, "A safety-based approaching behavioural model with various driving characteristics," *Transportation Research Part C: Emerging Technologies*, vol. 19, no. 6, pp. 1202–1214, 2011.

[11] G. J. Andersen and C. W. Sauer, "Optical information for car following: The driving by visual angle (DVA) model," *Human factors*, vol. 49, no. 5, pp. 878–896, 2007.

[12] S. Jin, D.-H. Wang, Z.-Y. Huang, and P.-F. Tao, "Visual angle model for car-following theory," *Physica A: Statistical Mechanics and its Applications*, vol. 390, no. 11, pp. 1931–1940, 2011.

[13] S. H. Hamdar, M. Treiber, H. S. Mahmassani, and A. Kesting, "Modeling driver behavior as sequential risk-taking task," *Transportation Research Record: Journal of the Transportation Research Board*, no. 2088, pp. 208–217, 2008.

[14] S. H. Hamdar, H. S. Mahmassani, and M. Treiber, "From behavioral psychology to acceleration modeling: Calibration, validation, and exploration of drivers' cognitive and safety parameters in a risk-taking environment," *Transportation Research Part B: Methodological*, vol. 78, pp. 32–53, 2015.

[15] B. S. Kerner, S. L. Klenov, and D. E. Wolf, "Cellular automata approach to three-phase traffic theory," *Journal of Physics A: Mathematical and General*, vol. 35, no. 47, pp. 9971–10013, 2002.

[16] W. Knospe, L. Santen, A. Schadschneider, and M. Schreckenberg, "Towards a realistic microscopic description of highway traffic," *Journal of Physics A: Mathematical and General*, vol. 33, no. 48, pp. L477–L485, 2000.

[17] J.-F. Tian, B. Jia, X.-G. Li, R. Jiang, X.-M. Zhao, and Z.-Y. Gao, "Synchronized traffic flow simulating with cellular automata model," *Physica A: Statistical Mechanics and its Applications*, vol. 388, no. 23, pp. 4827–4837, 2009.

[18] R. Jiang and Q. Wu, "First order phase transition from free flow to synchronized flow in a cellular automata model," *The European Physical Journal B-Condensed Matter and Complex Systems*, vol. 46, no. 4, pp. 581–584, 2005.

[19] J.-F. Tian, N. Jia, N. Zhu, B. Jia, and Z.-Z. Yuan, "Brake light cellular automaton model with advanced randomization for traffic breakdown," *Transportation Research Part C: Emerging Technologies*, vol. 44, pp. 282–298, 2014.

[20] L. Precht, A. Keinath, and J. F. Krems, "Effects of driving anger on driver behavior – Results from naturalistic driving data," *Transportation Research Part F: Traffic Psychology and Behaviour*, vol. 45, pp. 75–92, 2017.

[21] A. Sharma, Y. Ali, M. Saifuzzaman, Z. Zheng, and M. M. Haque, "Human Factors in Modelling Mixed Traffic of Traditional, Connected, and Automated Vehicles," in *Advances in Human Factors in Simulation and Modeling*, pp. 262–273, Springer, 2017.

[22] H. Zheng, C. Wu, and X. Ma, "Cellular automaton model for urban traffic flow considering driving anger," *Journal of Wuhan University of Technology (Transportation Science & Engineering)*, vol. 37, no. 3, pp. 617–621, 2013.

[23] J. Rong, K. Mao, and J. Ma, "Effects of individual differences on driving behavior and traffic flow characteristics," *Transportation Research Record: Journal of the Transportation Research Board*, no. 2248, pp. 1–9, 2011.

[24] G. Habtemichael Filmon and de Picado Santos Luis, "Safety Evaluations of Aggressive Driving on Motorways through Microscopic Traffic Simulation and Surrogate Measures," *Transportation Research Board 91st Annual Meeting, Transportation Research Board*, p. 17, 2012.

[25] G. Peng, H. He, and W.-Z. Lu, "A new car-following model with the consideration of incorporating timid and aggressive driving behaviors," *Physica A: Statistical Mechanics and its Applications*, vol. 442, pp. 197–202, 2016.

[26] X. Li, K. Fang, and G. Peng, "A new lattice model of traffic flow with the consideration of the drivers' aggressive characteristics," *Physica A: Statistical Mechanics and its Applications*, vol. 468, pp. 315–321, 2017.

[27] S. Sharma, "Lattice hydrodynamic modeling of two-lane traffic flow with timid and aggressive driving behavior," *Physica A: Statistical Mechanics and its Applications*, vol. 421, pp. 401–411, 2015.

[28] G. Zhang, D.-H. Sun, W.-N. Liu, M. Zhao, and S.-L. Cheng, "Analysis of two-lane lattice hydrodynamic model with consideration of drivers' characteristics," *Physica A: Statistical Mechanics and its Applications*, vol. 422, pp. 16–24, 2015.

[29] M. Zamith, R. C. P. Leal-Toledo, E. Clua, E. M. Toledo, and G. V. P. Magalhães, "A new stochastic cellular automata model for traffic flow simulation with drivers' behavior prediction," *Journal of Computational Science*, vol. 9, pp. 51–56, 2015.

[30] T. Q. Tang, J. He, S. C. Yang, and H. Y. Shang, "A car-following model accounting for the driver's attribution," *Physica A: Statistical Mechanics and its Applications*, vol. 1, pp. 583–591, 2014.

[31] Y. Zhang, P. Ni, M. Li, H. Liu, and B. Yin, "A new car-following model considering driving characteristics and preceding vehicle's acceleration," *Journal of Advanced Transportation*, vol. 2017, Article ID 2437539, 2017.

[32] R. Cheng, H. Ge, and J. Wang, "An extended continuum model accounting for the driver's timid and aggressive attributions," *Physics Letters A*, vol. 381, no. 15, pp. 1302–1312, 2017.

[33] R. Kang, L.-J. Peng, and K. Yang, "One-dimensional traffic cellular automaton model with consideration of the change of driving rules," *Acta Physica Sinica*, vol. 58, no. 7, pp. 4514–4522, 2009.

[34] H. Gartner Nathan, J. M. Carroll, and K. R. Ajay, *Monograph on traffic flow theory*, H. Gartner Nathan, J. M. Carroll, and K. R. Ajay, Eds., Federal Highway Administration, 1997.

[35] H. Wang, W. Wang, X. Chen, J. Chen, and J. Li, "Experimental features and characteristics of speed dispersion in urban freeway traffic," *Transportation Research Record*, vol. 1999, pp. 150–160, 2007.

[36] X. Qu, W. Wenfu, B. Ran, and D. Yunqi, "Quantitative Analysis of the Impact of Variable Speed Limits on Motorway Safety," *Transportation Research Board 96th Annual Meeting, Transportation Research Board*, 2017.